Atomic Spectroscopy

Article

Molybdenum Isotope Analysis Using the Neoma MS/MS MC-ICP-MS

Yan Han,[a] Feng Liang,[b,c,*] Zhifang Hu,[d] Lanping Feng,[a,*] Lian Zhou,[a] and Zhaochu Hu [a]

[a] State Key Laboratory of Geological Processes and Mineral Resources, China University of Geosciences, Wuhan 430074, P. R. China

[b] CNPC Key Laboratory of Carbonate Reservoirs, PetroChina Hangzhou Research Institute of Geology, Hangzhou 310023, P. R. China

[c] State Energy Key Laboratory for Carbonate Oil and Gas, PetroChina Hangzhou Research Institute of Geology, Hangzhou 310023, P. R. China

[d] Thermo Fisher Scientific (China), Shanghai 201206, P. R. China

Received: *October 15, 2025;* ***Revised:*** *December 05, 2025;* ***Accepted:*** *December 05, 2025;* ***Available online:*** *December 05, 2025.*

DOI: 10.46770/AS.2025.202

ABSTRACT: Molybdenum (Mo) isotopic analysis using multi-collector inductively coupled plasma mass spectrometry (MC-ICP-MS) has become a cornerstone technique in modern geochemistry. However, achieving accurate and precise measurements in samples with low Mo concentrations or complex matrices remains challenging due to conventional instrument limitations. This study presents the first systematic evaluation of the Thermo Scientific Neoma MS/MS MC-ICP-MS, a new and advanced platform featuring a double-Wien filter and an advanced collision/reaction cell (CRC) design, for Mo isotope measurements. We investigated how instrumental configurations—specifically cone combinations and plasma conditions—affect sensitivity and matrix tolerance, focusing on its potential to overcome existing analytical barriers. Compare to Neptune platform, the Neoma MS/MS exhibits markedly enhanced sensitivity, yielding a 2- to 5-fold improvement, under both dry and wet plasma conditions. Critically, a long-term external precision of 0.06‰ (2SD) at low concentrations, down to 10 ng g^{-1}, was achieved via Neoma. Notably, the Jet/X cone interface simultaneously enhances signal intensity and mitigates matrix effect, successfully challenging the conventional trade-off between sensitivity and matrix effect. These results highlight the Neoma MS/MS as a significant advancement for high-precision Mo isotope analysis, offering unprecedented accuracy and resilience under demanding geological conditions, particularly for samples with extremely low Mo content.

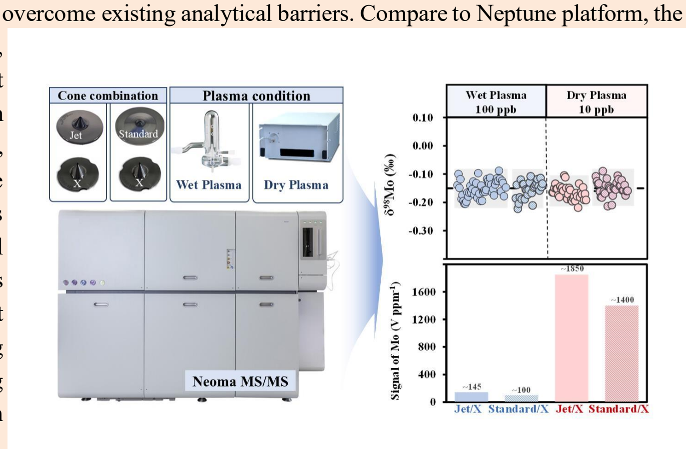

INTRODUCTION

Molybdenum (Mo), a transition metal, possesses seven stable isotopes, ^{92}Mo, ^{94}Mo, ^{95}Mo, ^{96}Mo, ^{97}Mo, ^{98}Mo and ^{100}Mo, with natural abundances of 14.84%, 9.25%, 15.92%, 16.68%, 9.55%, 24.13%, and 9.63%, respectively.[1] The isotopic composition of Mo has emerged as a powerful geochemical tracer with diverse applications, including paleo-environment reconstruction[2-4], the carbon cycle[5, 6], and planetary evolution[7].

Early determinations of Mo isotopic compositions were performed using thermal ionization mass spectrometry (TIMS) in the 1960s.[8, 9] However, these measurements suffered from large analytical uncertainty (~ ±6‰/amu) primarily due to the high ionization potential of Mo (7.1 eV), inefficient sample loading, potential isobaric interferences and instrumental isotopic fractionation. This limited Mo isotope studies until the late 1990s. The commercialization of the first multi-collector inductively coupled plasma mass spectrometry (MC-ICP MS), the Plasma 54 (VG Elemental, now Thermo Fisher Scientific, Bremen), marked a major breakthrough. This technological advance enabled high-precision Mo isotope ratio determinations, with intermediate precision levels of 0.03‰~0.08‰ (2SD) for $^{98}Mo/^{95}Mo$ being routinely achieved on commercially available MC-ICP-MS systems like the Neptune series (Thermo Fisher Scientific, Bremen, Germany) and Nu series (Nu Instruments, Wrexham, UK) instruments[10-16].

A further breakthrough occurred in 2018 when Nu Instruments launched the Sapphire dual Path MC-ICP-MS system incorporating a Collision/Reaction Cell (CRC). More recently, Thermo Fisher Scientific released the Neoma MS/MS MC-ICP-MS. This instrument is uniquely designed with an upgrade path to a MS/MS configuration featuring a CRC, which includes a unique pre-cell mass filter to select and transmit ions into the collision cell.[17] CRC technology enables separating analytes from isobaric interferences through chemical reactions. Interfering species are either neutralized or converted into a different product molecule with a distinct mass-to-charge ratio. However, complex sample matrices can introduce unpredictable reactions within the CRC, leading to the generation of new interfering species and chaotic conditions. To better control the reactions inside the CRC, a pre-cell mass filter is employed to preselect a specific mass range of ions to enter the cell. This approach prevents a large portion of the sample matrix and the major Argon ion beam from entering the cell. This effectively prevents the formation of molecular interferences, cleans up the mass spectra, and ensures interference-free detection of the analyte.[17, 18] Current technological trajectories suggest that MC-ICP-MS with CRC systems will become the dominant platform for high-precision isotope ratio measurements, progressively replacing previous-generation instruments. The Neoma MS/MS MC-ICP-MS has already demonstrated robust analytical performance for several light-to-medium mass elements, including validated applications for Sr[19, 20], Cu[21], K[22, 23] and Li[24]. However, its performance for Mo isotopic analysis has not yet been systematically evaluated, particularly concerning its sensitivity and matrix effects.

The main objective of this study is therefore to conduct the first comprehensive assessment of the Neoma MS/MS MC-ICP-MS for Mo isotope analysis. Specifically, we aim to investigate how different instrumental configurations—including cone combinations and plasma conditions—affect analytical sensitivity and matrix effects. These results provide critical insights necessary for optimizing measurement precision and accuracy for high-precision Mo isotope determinations using this next-generation MC-ICP-MS instrument.

EXPERIMENTAL

All chemical procedures were completed in laminar flow work hoods (class 100) installed in a clean room (class 1000) at the State Key Laboratory of Geological Processes and Mineral Resources (GPMR), China University of Geosciences (Wuhan).

Reagents and materials. Nitric acid (HNO_3, analytical grade) used in this study was purified twice by sub-boiling distillation prior to use. Deionized water (DI water, 18.2 MΩ cm) used throughout all experimental procedures was produced by Milli-Q series ultrapure water system (Millipore Corporation, US). The NIST SRM 3134 molybdenum standard solution (lot # 130418), obtained from the National Institute of Standards and Technology (USA), was used as the '$\delta^{98}Mo = 0$' reference material for Mo isotope analysis. A commercially available Mo standard solution, Alfa Mo (Alfa Aesar, UK), was analyzed periodically to monitor the long-term reproducibility of isotope measurements. A ^{97}Mo-^{100}Mo double spike solution was prepared from the highly enriched ^{97}Mo and ^{100}Mo isotopes supplied by Oak Ridge National Laboratory (ORNL, USA), and was calibrated relative to NIST SRM 3134 Mo in previous study by Feng et al.[16] A series of mono-elemental ICP standards including Fe, Ti, Co, Ni, Sr, and Ru (all 1000 μg mL^{-1}) were obtained from the National Analysis Center for Iron and Steel (NACIS; Beijing, China).

Isotopic analyses. The Mo isotopic analyses were carried out on the Neoma MS/MS MC-ICP-MS at the GPMR. This instrument is equipped with eleven Faraday cups connected to 10^{11} Ω amplifiers. Two types of cone combinations were employed: a Standard sample cone and X skimmer cone (hereafter "Standard/X") and a Jet sample cone and X skimmer cone (hereafter "Jet/X"). Sample were introduced into the plasma via a 50 μL min^{-1} PFA nebulizer connected to a CETAC ASX-112FR autosampler. The introduction system consisted of either a dual cyclonic double-pass spray chamber in wet plasma mode, or an Aridus III desolvating system (Teledyne CETAC Technologies, Omaha, USA) in dry plasma mode. The Neoma MS/MS is controlled using the Qtegra ISDS software. The Mo isotope ratio measurements were performed in static mode at low mass resolution. The isotopes ^{92}Mo, ^{94}Mo, ^{95}Mo, ^{96}Mo, ^{97}Mo, ^{98}Mo and ^{100}Mo were simultaneously collected by Faraday cups positioned at L3, L2, L1, C, H1, H2 and H4, respectively. The isobaric interferences from Zr and Ru were monitored by collecting ^{91}Zr in L4 and ^{99}Ru in H3.

Before starting the Mo isotope ratio measurements, the Neoma MS/MS MC-ICP-MS settings were carefully optimized to ensure attainment of the maximum signal intensity and stability for ^{98}Mo for both Standard/X and Jet/X, respectively. For the wet plasma modes, the $^{98}Mo^+$ signal intensities could achieve ~5 V and ~7 V in a 200 ng g^{-1} NIST SRM 3134 solution using Standard/X and Jet/X, respectively. For the dry plasma modes, the $^{98}Mo^+$ signal intensities could achieve ~17V and ~22 V in a 50 ng g^{-1} NIST SRM 3134 solution using Standard/X and Jet/X, respectively.

Each analysis consisted of a 120 s wash, 60 s uptake, and 120 s measurement (30 cycles of 4.194 s integration). The blank levels in the 5% (w/w) HNO_3 solutions were observed to be lower than 1mV on Mo isotopes, and ~0.01mV on ^{90}Zr and ^{99}Ru. To monitor

Table 1. Typical tuning settings of Neoma MS/MS used for Mo isotopic measurements

Parameter	Value
Source Slit	Low resolution
Peristaltic Pump Speed (rpm)	40
Plasma Power (W)	1200
Torch Horizontal Position (mm)	~1
Torch Vertical Position (mm)	~1
Torch Sampling Depth (mm)	~5.6
Auxiliary Gas Flow (l/min)	~1
Nebulizer Gas Flow (l/min)	~1.25
Electric Field (V)	110
Magnetic Field (%)	20
Slit Opening (%)	100
Lens Supply L1-Base (V)	~ -440
Lens Supply L2-Base (V)	~ -425
Lens Supply L3-Base (V)	~ -400
MSMS CCT Entry (V)	~ -30
CCT Bias (V)	0
MSMS CCT Exit 1 (V)	~ -100
MSMS CCT Exit2 (V)	~ -89
MSMS CCT RF Amplitude (%)	100
Focus (%)	45
Shape (%)	62
Aridus III- Ar (L/min) (dry plasma mode)	~4.0
Aridus III- N_2 (mL/min) (dry plasma mode)	~2

any change in blank levels and their potential influence on Mo isotope measurements, acid blanks were measured before and after each sample or standard, following the same procedure. The δ^{98}Mo values for each sample reported in this study represent the average of more than three replicate analyses. The typical operating conditions are summarized in Table 1. Instrumental mass bias was corrected using a combined double-spike and standard-sample bracketing (SSB) technique[16, 25]. Mo isotopic ratios were reported in standard δ-notation in per mil relative to standard reference material NIST SRM 3134:

$$\delta^{98}\text{Mo} = [(^{98}\text{Mo}_{\text{sample}}/^{95}\text{Mo}_{\text{sample}}) / (^{98}\text{Mo}_{\text{NIST SRM 3134}}/^{95}\text{Mo}_{\text{NIST SRM 3134}})-1] \times 1000 \quad (1)$$

RESULTS AND DISCUSSION

Signal sensitivity. High-precision isotope ratio analysis relies fundamental on superior instrumental sensitivity, which enhances the signal-to-noise ratio by increasing the ion beam intensity.[26] In MC-ICP-MS, both analytical accuracy and precision are influenced by a suite of parameters—including gas flows, plasma position, RF power, and lens focusing—all of which are routinely optimized prior to measurement. Beyond these settings, the configuration of the sample introduction system and the cone interface exert a decisive influence on overall performance, as they collectively determine the signal intensity, stability, and ultimately the efficiency of ionization and ion transmission. [27-29]

The sensitivity for Mo was evaluated using a pure NIST SRM 3134 standard solution. As summarized in Table 2, under wet plasma conditions, sensitivities of approximately 100 V ppm^{-1} and 145 V ppm^{-1} were obtained using the Standard/X and Jet/X cone configurations, respectively. In contrast, under dry plasma conditions, sensitivity increased markedly to around 1400 V ppm^{-1} and 1850 V ppm^{-1} for the same cone sets, representing a 12- to 14-fold enhancement relative to wet plasma measurements. When compared with previously reported values obtained under consistent sample introduction conditions (50 μL min^{-1} nebulizer flow rate), the Neoma MS/MS demonstrates clearly superior sensitivity. In wet plasma mode, the sensitivity exceeded that of the typical Neptune series (~33 V ppm^{-1} for Mo[30, 31]) by a factor of 3–5. In dry plasma mode, where Neptune and Nu series instruments typically achieve 100–1050 V ppm^{-1},[13-16, 25, 32-40] the Neoma MS/MS series consistently delivered values more than twice as high.

This enhanced sensitivity can be primarily attributed to the double Wien pre-cell mass filter and the newly designed robust ICP source. By adjusting the electric and magnetic fields of the double-Wien filter, effective suppression of argon-derived ions is achieved. This significantly reduces space charge effects which are caused by high-density ion beams that lead to Coulombic repulsion and defocusing of the ion beam, particularly detrimental to the transmission of medium mass analyte ions. The removal of these interfering ions thus reduces space charge defocusing, thereby significantly improving the focusing and transmission efficiency for Mo^+. As previously reported by Télouk *et al.*[21], even without activating the CRC, basic tuning of the magnetic and electric fields in the double Wien filter significantly affects ion transmission in the low-mass range. With the adjustable slit fully open (S = 100%) and the magnetic field set to its minimum value (B = 10%), the system nearly completely suppresses argon-derived signals while maintaining highly efficient transmission of high-mass ions. Further increasing the magnetic field to 20% and 30% successively eliminates the transmission of species in the 40-70 amu range and enhances ion transmission efficiency around the target mass, consistent with a reduction in space charge effect.

Effect of acid concentration mismatch. Previous studies have indicated that different nitric acid concentrations between samples or standards can introduce artifacts in metal stable isotope analysis.[41-44] To assess the impact of acid concentration mismatch on Mo isotope measurements using Neoma MS/MS, a series of experiments were conducted in this study. NIST SRM 3134 solutions, spiked with 45% ^{97}Mo-^{100}Mo double spike solution, were prepared at varying HNO_3 concentrations (1%–9%, w/w) and measured against a NIST SRM 3134 Mo solution in 5% HNO_3, covering sample-to-standard acid concentration ratios from 0.2 to 1.8 (Fig. 1).

Table 2. Summary of Mo isotope sensitivity under different testing conditions and instruments

Reference	Instrument	Cone combination	Plasma	Nebulizer flow (μL min^{-1})	Sensitivity (V ppm^{-1})
Archer and Vance[32]	Neptune	——[f]	dry	——	180-200
Pearce et al.[33]	Nu	——	dry	80	~140[a]
Wen et al.[34]	Nu Plasma	——	dry	100	~57[a]
Goldberg et al.[35]	Nu Plasma HR	——	dry	100	160-240[a]
Li et al.[14]	Neptune Plus	Standard/X	dry	——	180-200[a]
Malinovsky et al.[30]	Neptune	——	wet	——	~33[b]
Skierszkan et al.[36]	Nu Plasma	——	dry	——	~100-180[c]
Liu et al.[15]	Neptune Plus	Standard/X	dry	50	~300[a]
Willbold et al.[37]	Neptune	Standard/H	dry	50	~250[d]
Zhao et al.[38]	Neptune Plus	——	dry	——	180-200[a]
Fan et al.[31]	Neptune Plus	Standard/X	wet	50	~34[b]
Feng et al.[16]	Neptune Plus	Jet/X	dry	50	410-580[b]
Gaspers et al.[39]	Neptune	Standard/X	dry	30	600-840[e]
Zhang et al.[40]	Neptune Plus	Standard/X	dry	50	180-200[a]
Zhu et al.[13]	Neptune Plus	Standard/X	dry	110	1250-2070[d]
Zhu et al.[13]	Nu II	541B (1.15 mm)/dry cone (0.9 mm), 540 (0.6 mm orifice)/dry cone	dry	100	125-220[d]
Han et al.[25]	Neptune Plus	Jet/X	dry	50	~ 830[b]
In this study	Neoma MS/MS	Standard/X	wet	50	~100[b]
In this study	Neoma MS/MS	Standard/X	dry	50	~1400[b]
In this study	Neoma MS/MS	Jet/X	wet	50	~145[b]
In this study	Neoma MS/MS	Jet/X	dry	50	~1850[b]

Note: [a] the sensitivity for Mo is reported directly in the literature without conversion; [b] the sensitivity for Mo is based on the ^{98}Mo in the literature with conversion; [c] the sensitivity for Mo is based on the ^{94}Mo in the literature with conversion; [d] the sensitivity for Mo is based on the ^{95}Mo in the literature with conversion; [e] the sensitivity for Mo is based on the ^{96}Mo in the literature with conversion; [f] denotes that the corresponding data are not reported in the literature.

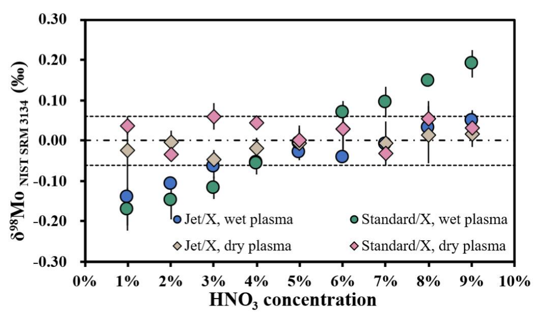

Fig. 1 Effect of HNO_3 concentrations on the Mo isotopic analysis by the Neoma MS/MS MC-ICP-MS. The area between two dotted lines denotes the typical analytical uncertainty for Mo isotope ratios (±0.07‰, Table S1).

A notable influence of acid concentration mismatch on isotopic compositions was observed in wet plasma mode. As shown in Fig. 1. Using Standard/X, δ^{98}Mo values increased from –0.17‰ to +0.19‰ as the HNO_3 concentration rose from 1% to 9% (w/w), highlighting the necessity of strict acid concentration matching between samples and bracketing standard solutions. Jet/X was less sensitive to acidity under wet plasma conditions; however, it was still necessary to maintain acid concentrations of samples within 4% to 9% HNO_3.

In contrast, dry plasma mode with both cone combinations showed negligible sensitivity to variations in acid concentration. Measured δ^{98}Mo values remained consistent at 0.00 ± 0.07‰ (2SD, Table S1) across the 1% to 9% HNO_3 range, confirming that the desolvating nebulizer effectively removed solvent-related matrix effects. Nonetheless, samples and standards were diluted using the same batch of 5% HNO_3 during the measurements to ensure elimination of acidity-related effects.

Effect of Mo concentration mismatch. Previous studies have shown that concentration mismatch between samples and bracketing standards can cause analytical inaccuracies in double-spike analysis.[45, 46] To assess the influence of Mo concentration mismatch on isotope measurements using the Neoma MS/MS MC-ICP-MS, we analyzed a series of diluted NIST SRM 3134 solutions (each spiked with 45% ^{97}Mo–^{100}Mo double spike) against a NIST SRM 3134 bracketing standard. Solutions were prepared at typical concentrations for wet and dry plasma modes, 200 ng g^{-1} and 50 ng g^{-1} Mo, respectively.

The results of the concentration-matching experiments are summarized in Fig. 2 and Table S2. Under wet plasma conditions using both Jet/X and Standard/X cones, as well as under dry plasma conditions with the Jet/X cone, measured Mo isotope ratios exhibited negligible variation across a sample-to-standard concentration ratio range of 0.2 to 1.8. This demonstrates that the standard-sample bracketing method, combined with double-spike correction, is robust in accommodating moderate concentration mismatches. However, when using the Standard/X cones in dry plasma mode, a pronounced isotopic fractionation exceeding 0.14‰ was observed at sample-to-standard concentration ratios above 1.6. This observed fractionation is likely due to enhanced space charge effects[29]. The larger orifice diameter of the sample cone permits more ions to enter the interface. Under dry plasma conditions,

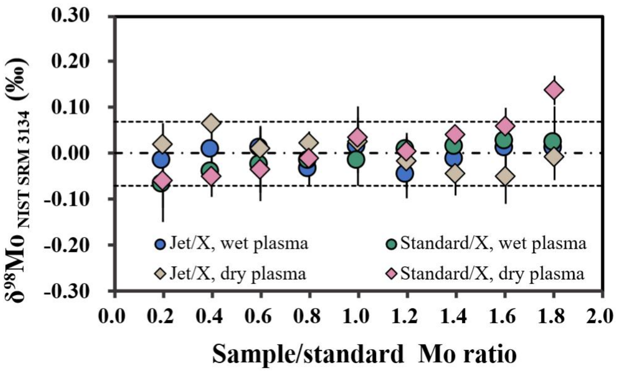

Fig. 2 Effects of double spike proportion on the Mo isotopic analysis by the Neoma MS/MS MC-ICP-MS. The area between two dotted lines denotes the typical analytical uncertainty for Mo isotope ratios (±0.07‰, Table S2).

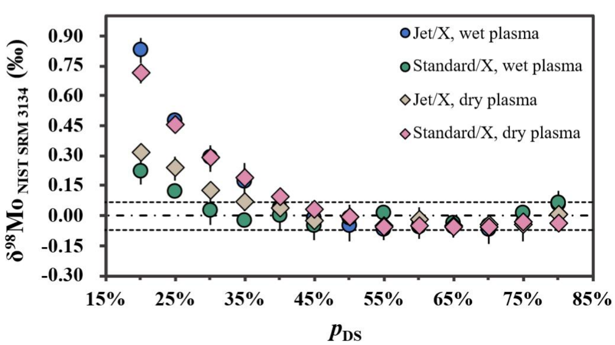

Fig. 3 Effects of double spike proportion on the Mo isotopic analysis by the Neoma MS/MS MC-ICP-MS. The area between two dotted lines denotes the typical analytical uncertainty for Mo isotope ratios (±0.07‰, Table S3).

higher Mo concentration (exceeding sample-to-standard ratio >1.6) lead to strong Coulomb repulsion behind the cone orifice. Under these conditions, lighter isotopes are preferentially scattered from the ion beam, while heavier isotopes are transmitted more efficiently, resulting in the observed isotopic bias. As a precaution all Mo isotope analyses were performed with sample concentrations maintained within 5% of the bracketing standards.

Effect of double spike proportion. The double spike proportion (hereafter "p_{DS}", p_{DS} = double spike/ (sample + double spike)) can influence both the precision and accuracy of measured Mo isotope ratios by affecting mass bias correction efficiency and signal intensity optimization.[47] To evaluate the effect of p_{DS} on the Mo isotope measurement using the Neoma MS/MS MC-ICP-MS, NIST SRM 3134 Mo solutions (200 ng g^{-1} for wet plasma mode and 50 ng g^{-1} for dry plasma mode) were spiked with varying amounts of ^{97}Mo–^{100}Mo double spike, covering a p_{DS} range of 20% to 80% (Fig. 3 and Table S3).

Results show that insufficient double spike addition (p_{DS} < 30%) leads to significant δ^{98}Mo deviations (> 0.12‰) from the true value of 0‰. The optimal p_{DS} range for accurate measurement—where results fall within the analytical uncertainty of ±0.07‰—depends on the instrumental configuration. In wet plasma mode, acceptable accuracy was achieved at p_{DS} 30%-80% with Standard/X cones and 40%-80% with Jet/X cones. Under dry plasma conditions, the suitable p_{DS} range was 35%-80% for Jet/X and 45%-80% for Standard/X. Based on these results, a p_{DS} value of 45% was selected for all subsequent high-precision Mo isotope measurements in this study, as it lies within the optimal range for all configurations and ensures robust, reproducible analytical performance.

Spectral interferences on the ^{98}Mo/^{95}Mo ratio. In Mo isotope analysis, sample matrices can affect measurements through non-spectral and spectral interferences. Spectral interferences primarily arise from isobaric interferences, doubly charged ion interferences, and polyatomic ion interferences. Critical spectral interferences on Mo include Fe, Co, Ni, Sr, and Ru.[25] Although chemical purification effectively removes most matrix elements, residual trace species—particularly those inducing spectral interferences—can still compromise high-precision Mo isotope determinations. We therefore systematically evaluated matrix effects during Mo isotope measurements on the Neoma MS/MS MC-ICP-MS.

Different amounts of matrix elements (Fe, Co, Ni, Sr, and Ru) were added to NIST SRM 3134 standard solutions spiked with 45% ^{97}Mo-^{100}Mo double spike solution. Results indicated stronger matrix effects under the dry plasma conditions compared to wet plasma conditions (Fig. 4 and Table S4). Under dry plasma mode with Standard/X, δ^{98}Mo exhibited positive deviations (δ^{98}Mo > +0.12‰) at critical elemental ratios: Fe/Mo > 1, Ni/Mo > 0.1, and Co/Mo > 0.05. Conversely, Sr introduced measurable negative offsets (δ^{98}Mo < -0.18‰) when Sr/Mo exceeded 2. The Jet/X cone configuration in dry plasma mode showed greater matrix tolerance, significant deviations occurred only when Ni/Mo > 0.1, Co/Mo > 0.1, and Sr/Mo > 2, while δ^{98}Mo remained unaffected at Fe/Mo ratio ≤10.

Under wet plasma mode, the Standard/X cone combination was more susceptible to matrix effects than Jet/X. Standard/X measurements showed positive δ^{98}Mo anomalies (δ^{98}Mo > 0.09‰) at Fe/Mo > 1, Ni/Mo > 0.1, or Co/Mo > 0.05, and negative deviations (δ^{98}Mo < -0.32‰) at Sr/Mo > 2. When employing the Jet/X in the wet plasma mode, Mo isotope measurements remained consistent with true value within ±0.07‰ (2SD) at Fe/Mo ≤ 10, Ni/Mo ≤ 0.1, Co/Mo ≤ 0.1, and Sr/Mo ≤ 2.

Compared to wet plasma conditions, dry plasma, which is solvent-free, produces a more concentrated ion beam. This not only increases the absolute signal of interferents, but also, more critically, intensifies space charge effects at the interface, leading to matrix-dependent beam divergence and mass fractionation, making dry plasma inherently more susceptible to matrix effects. Across all four conditions, uncorrected Ru isobaric interference

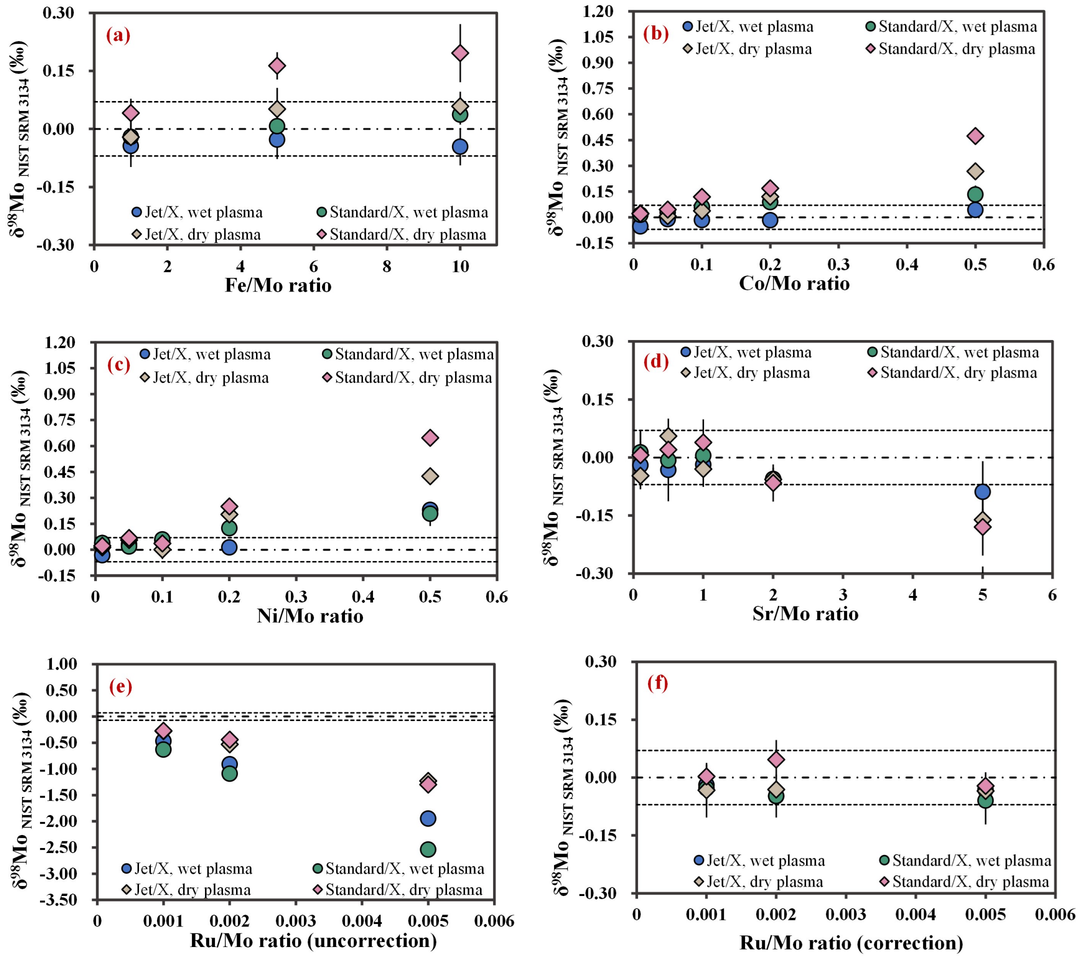

Fig. 4 Spectral interferences on the Mo isotopic analysis by the Neoma MS/MS MC-ICP-MS. The area between two dotted lines denotes the typical analytical uncertainty for Mo isotope ratios (±0.07‰, Table S4)

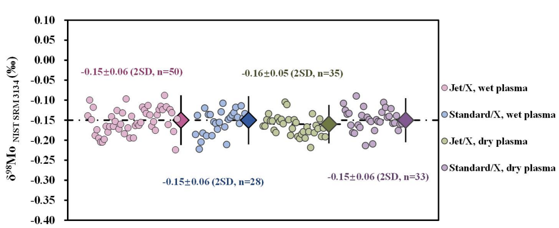

Fig. 5 Long-term (ca. three months) analyses of Alfa Mo solution relative to NIST SRM 3134. The long-term external precision (2SD) is better than 0.06‰.

induced substantial negative δ^{98}Mo biases (> 0.25‰) at Ru/Mo = 0.001. Applying the interference correction method of Feng *et al.*[48] effectively mitigated the isobaric effect, yielding δ^{98}Mo within negligible deviation from reference values for Ru/Mo ≤ 0.005.

Overall, the Jet/X cone configuration provided superior analytical performance for Mo isotope ratio determination using Neoma MS/MS MC-ICP-MS.

Precision and accuracy. The precision and accuracy of the Mo isotopic analysis were assessed by repeated measurements of Alfa Mo standard solutions against the NIST SRM 3134 reference standard. These solutions, spiked with 45% ^{97}Mo-^{100}Mo double spike solution, were prepared at 100 ng g^{-1} (wet plasma) and 10 ng g^{-1} (dry plasma) in 5% HNO_3 (w/w). Within-run precision (2SE) for the ^{98}Mo/^{95}Mo ratio ranged from 0.02 to 0.06‰. External precision was monitored by analyzing the Alfa Mo solutions and bracketing NIST SRM 3134 standard solutions over a three-month period (September–December 2024; Fig. 5 and Table S5).

Long-term δ^{98}Mo values for Alfa Mo were -0.15 ± 0.06‰ (2SD, n=50) in wet plasma mode with Jet/X, -0.15 ± 0.06‰ (2SD, n=28) in wet plasma mode with Standard/X, -0.16 ± 0.05‰ (2SD, n=35) in dry plasma with Jet/X and -0.15 ± 0.06‰ (2SD, n=33) in dry plasma with Standard/X (Fig. 5). These results are consistent with previously reported values of -0.15 ± 0.08‰ (n=46, 2SD) by Eroglu *et al.* [49] and -0.17 ± 0.03‰ (n=55, 2SD) by King *et al.*[50] .

Notably, the high precision achieved at 10 ng g^{-1} in dry plasma mode demonstrates the method's capability for reliable analysis of samples with ultra-low Mo contents, significantly expanding the applicability of Mo isotope analysis in geochemical studies.

CONCLUSION

This study systematically evaluated the performance of the Neoma MS/MS MC-ICP-MS for Mo isotope analysis under varying cone configurations and plasma conditions, focusing on instrumental sensitivity and key matrix-related effects, including acid and Mo concentration mismatch, double-spike proportion, and elemental interferences.

The Neoma MS/MS demonstrated markedly improved sensitivity compared with previously reported instruments, achieving enhancements of approximately 3-5 and 2-4 times under wet and dry plasma conditions, respectively. Our results further revealed that dry plasma conditions effectively suppress matrix effects arising from acid concentration variations (1%-9%), whereas such effects remain pronounced under wet plasma, particularly with the Standard/X cone. Mo concentration mismatch introduced negligible bias within a sample-to-standard ratio range of 0.2-1.8 for most configurations, except under wet plasma with the Standard/X interface. The optimal double-spike proportion for the Jet/X configuration under dry plasma conditions was identified as 35%-80%, ensuring an optimal balance between analytical precision and robustness.

While dry plasma considerably enhances sensitivity, it also amplifies matrix effect, which were consistently more severe with Standard/X cones than with Jet/X cones. Notably, the Jet/X cone combined with dry plasma yielded the highest sensitivity (~1850 V ppm^{-1}) and remarkable long-term reproducibility (0.05‰ for 10 ng g^{-1} Mo). Importantly, this configuration not only achieved higher signal intensity but also minimized matrix effects, revising previous understanding based on earlier generations of instrumentation. These performance advantages establish the Neoma MS/MS as a powerful and reliable platform for high-precision Mo isotope analysis in geochemical samples with low Mo contents and complex matrices.

ASSOCIATED CONTENT

The supporting information (Tables S1-S5) is available at https://www.at-spectrosc.com.

AUTHOR INFORMATION

Feng Liang received his Ph.D. in geochemistry from the Institute of Geochemistry, Chinese Academy of Sciences in 2018. Since 2018, he worked as a geochemist at the PetroChina Hangzhou Research Institute of Geology. His research focuses on development and application of laser ablation U-Pb dating and non-traditional isotope analytical techniques.

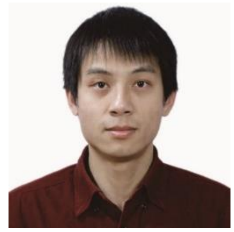

Lanping Feng earned his M.S. (2012) and Ph.D. (2016) in Geochemistry from the China University of Geosciences, Wuhan. He is currently an Associate Researcher at the State Key Laboratory of Geological Processes and Mineral Resources, China University of Geosciences, Wuhan. His research focuses on analytical methodologies for non-traditional stable isotopes, with innovative contributions to sample pretreatment protocols, mass-dependent fractionation correction strategies, and isotope data reduction techniques. He has authored or co-authored more than 50 peer-reviewed SCI publications.

Corresponding authors

* F. Liang

E-mail address: liangf_hz@petrochina.com.cn

* L. P. Feng

E-mail address: ucg1987@163.com

Notes

The authors declare no competing financial interest.

ACKNOWLEDGMENTS

This work was financially supported by the National Natural Science Foundation of China (42373031) and the National Natural Science Foundation of China Joint Fund for Enterprise Innovation and Development (U23B20154).

REFERENCES

1. M. Willbold and T. Elliott, *Chem. Geol.*, 2017, **449**, 253-268. https://doi.org/10.1016/j.chemgeo.2016.12.011
2. E. M. O'Sullivan, T. F. Nägler, E. C. Turner, B. S. Kamber, M. G. Babechuk, and S. P. O'Hare, *Precambrian Res.*, 2022, **378**, 106760. https://doi.org/10.1016/j.precamres.2022.106760
3. M. Thoby, K. O. Konhauser, P. W. Fralick, W. Altermann, P. T. Visscher, and S. V. Lalonde, *Geology*, 2019, **47**, 559-562. https://doi.org/10.1130/g45706.1
4. A. J. Dickson, *Nat. Geosci.*, 2017, **10**, 721-726. https://doi.org/10.1038/ngeo3028
5. R. M. Gaschnig, C. T. Reinhard, N. J. Planavsky, X. Wang, D. Asael, and C. Chauvel, *Geochem., Geophys., Geosyst.*, 2017, **18**, 4674-4689. https://doi.org/10.1002/2017gc007085
6. Y. Zhang, C. Yuan, M. Sun, J. Li, X. Long, Y. Jiang, and Z. Huang, *Geochim. Cosmochim. Acta*, 2020, **278**, 340-352. https://doi.org/10.1016/j.gca.2019.12.013
7. Q. Yin, S. B. Jacobsen, and K. Yamashita, *Nature*, 2002, **415**, 881-883. https://doi.org/10.1038/415881a

8. V. R. Murthy, *J. Geophys. Res.:Solid Earth*, 1962, **67**, 905-907. https://doi.org/10.1029/JZ067i003p01161
9. G. W. Wetherill, *J. Geophys. Res.*, 1964, **69**, 4403-4408. https://doi.org/10.1029/JZ069i020p04403
10. D. Malinovsky, I. Rodushkin, D. C. Baxter, J. Ingri, and B. Öhlander, *Int. J. Mass Spectrom.*, 2005, **245**, 94-107. https://doi.org/10.1016/j.ijms.2005.07.007
11. A. J. Pietruszka, R. J. Walker, and P. A. Candela, *Chem. Geol.*, 2006, **225**, 121-136. https://doi.org/10.1016/j.chemgeo.2005.09.002
12. Y. Nakagawa, M. L. Firdaus, K. Norisuye, Y. Sohrin, K. Irisawa, and T. Hirata, *Anal Chem*, 2008, **80**, 9213-9219. https://doi.org/10.1021/ac801383t
13. H. G. Zhu, J. M. Zhu, D. Tan, X. Lin, K. Lu, and W. Yang, *J. Anal. At. Spectrom.*, 2022, **37**, 1063-1075. https://doi.org/10.1039/d1ja00465d
14. J. Li, X. R. Liang, L. F. Zhong, X. C. Wang, Z. Y. Ren, S. L. Sun, Z. F. Zhang, and J. F. Xu, *Geostand. Geoanal. Res.*, 2014, **38**, 345-354. https://doi.org/10.1111/j.1751-908X.2013.00279.x
15. J. Liu, H. J. Wen, Y. X. Zhang, H. F. Fan, and C. W. Zhu, *J. Anal. At. Spectrom.*, 2016, **31**, 1287-1297. https://doi.org/10.1039/c6ja00006a
16. L. Feng, L. Zhou, W. Hu, W. Zhang, B. Li, Y. Liu, Z. Hu, and L. Yang, *J. Anal. At. Spectrom.*, 2020, **35**, 145-154. https://doi.org/10.1039/c9ja00267g
17. T. F. Scientific. Thermo Fisher Scientific, 2020. https://www.thermofisher.cn/order/catalog/product/IQLAAMGAATFARHMBNK?icid=CMD_PDP_Neoma-to-NeomaMSMS
18. P. Télouk, E. Albalat, T. Tacail, F. Arnaud-Godet, and V. Balter, *J. Anal. At. Spectrom.*, 2022, **37**, 1259-1264. https://doi.org/10.1039/d2ja00050d
19. N. Dauphas, T. Hopp, G. Craig, Z. J. Zhang, M. C. Valdes, P. R. Heck, B. L. A. Charlier, E. A. Bell, T. M. Harrison, A. M. Davis, L. Dussubieux, P. R. Williams, M. J. Krawczynski, C. Bouman, N. S. Lloyd, D. Tollstrup, and J. B. Schwieters, *J. Anal. At. Spectrom.*, 2022, **37**, 2420-2441. https://doi.org/10.1039/d2ja00135g
20. P. Télouk and V. Balter, *J. Anal. At. Spectrom.*, 2024, **39**, 879-887. https://doi.org/10.1039/d3ja00358b
21. P. Télouk, E. Albalat, B. Bourdon, F. Albarède, and V. Balter, *J. Anal. At. Spectrom.*, 2023., 38, 1973-1983. https://doi.org/10.1039/d3ja00182b
22. E. Albalat, P. Télouk, and V. Balter, *J. Anal. At. Spectrom.*, 2024, **39**, 2183-2191. https://doi.org/10.1039/d4ja00211c
23. N. X. Nie, R. Grigoryan, and F. L. H. Tissot, *J. Anal. At. Spectrom.*, 2024, **39**, 2038-2048. https://doi.org/10.1039/d4ja00133h
24. S. R. Scott, G. L. Turner, B. N. Gartman, S. A. Anguiano, K. M. Melby, B. E. Allen, T. D. Minton, M. A. RisenHuber, and K. P. Hobbs, *J. Anal. At. Spectrom.*, 2025, **40**, 1098-1105. https://doi.org/10.1039/d4ja00419a
25. Y. Han, L. Zhou, A. Hu, L. Feng, A. Shen, and Z. Hu, *Anal. Chim. Acta*, 2025, **1375**, 344566. https://doi.org/10.1016/j.aca.2025.344566
26. Z. J. Zhang, N. X. Nie, and C. Z. Lin, *J. Anal. At. Spectrom.*, 2025, **40**, 2945-2956. https://doi.org/10.1039/d5ja00189g
27. Y. Yu, C. Siebert, J. Fietzke, T. Goepfert, E. Hathorne, Z. Cao, and M. Frank, *Chem. Geol.*, 2020, **549**, 119697. https://doi.org/10.1016/j.chemgeo.2020.119697
28. L.-F. Gou, Z.-D. Jin, L. Deng, M.-Y. He, and C.-Y. Liu, *Spectrochim. Acta B*, 2018, **146**, 1-8. https://doi.org/10.1016/j.sab.2018.04.015
29. M. He, Z. Jin, H. Lu, L. Deng, and C. Luo, *Int. J. Mass Spectrom.*, 2016, **408**, 33-37. https://doi.org/10.1016/j.ijms.2016.08.010
30. D. Malinovsky and F. Vanhaecke, *J. Anal. At. Spectrom.*, 2014, **29**, 1090-1097. https://doi.org/10.1039/c4ja00013g
31. J. J. Fan, J. Li, Q. Wang, L. Zhang, J. Zhang, X. L. Zeng, L. Ma, and Z. L. Wang, *Chem. Geol.*, 2020, **545**, 119648. https://doi.org/10.1016/j.chemgeo.2020.119648
32. C. Archer and D. Vance, *Nat. Geosci.*, 2008, **1**, 597-600. https://doi.org/10.1038/ngeo282
33. C. R. Pearce, A. S. Cohen, and I. J. Parkinson, *Geostand. Geoanal. Res.*, 2009, **33**, 219-229. https://doi.org/10.1111/j.1751-908X.2009.00012.x
34. H. J. Wen, J. Carignan, C. Cloquet, X. K. Zhu, and Y. X. Zhang, *J. Anal. At. Spectrom.*, 2010, **25**, 716-721. https://doi.org/10.1039/B921060A
35. T. Goldberg, G. Gordon, G. Izon, C. Archer, C. R. Pearce, J. McManus, A. D. Anbar, and M. Rehkämper, *J. Anal. At. Spectrom.*, 2013, **28**, 724-735. https://doi.org/10.1039/c3ja30375f
36. E. K. Skierszkan, M. Amini, and D. Weis, *Anal. Bioanal. Chem.*, 2015, **407**, 1925-1935. https://doi.org/10.1007/s00216-014-8448-6
37. M. Willbold, K. Hibbert, Y.-J. Lai, H. Freymuth, R. C. Hin, C. Coath, F. Vils, and T. Elliott, *Geostand. Geoanal. Res.*, 2016, **40**, 389-403. https://doi.org/10.1111/ggr.12109
38. P. P. Zhao, J. Li, L. Zhang, Z. B. Wang, D. X. Kong, J. L. Ma, G. J. Wei, and J. F. Xu, *Geostand. Geoanal. Res.*, 2016, **40**, 217-226. https://doi.org/10.1111/j.1751-908X.2015.00373.x
39. N. Gaspers, T. Magna, and L. Ackerman, *Geostand. Geoanal. Res.*, 2020, **44**, 363-374. https://doi.org/10.1111/ggr.12314
40. J. Zhang, J. Li, L. Zhang, Z.-b. Wang, S.-l. Sun, and Z.-y. Luo, *Rapid Commun. Mass Spectrom.*, 2020, **34**, e8658. https://doi.org/10.1002/rcm.8658
41. W. Hu, L. Chen, X. Geng, Z. Liang, and S. Tian, *Talanta*, 2025, **283**, 127122. https://doi.org/10.1016/j.talanta.2024.127122
42. J. Wang, D.-M. Tang, B.-X. Su, Q.-H. Yuan, W.-J. Li, B.-Y. Gao, K.-Y. Chen, Z.-A. Bao, and Y. Zhao, *J. Anal. At. Spectrom.*, 2022, **37**. 1869-1875. https://doi.org/10.1039/d2ja00084a
43. H.-O. Gu and H. Sun, *J. Anal. At. Spectrom.*, 2021, **36**, 2545-2552. https://doi.org/10.1039/d1ja00201e
44. Y. Zhang, Z. Bao, N. Lv, K. Chen, C. Zong, and H. Yuan, *Front Chem*, 2020, **8**, 609. https://doi.org/10.3389/fchem.2020.00609
45. J.-X. She, W. Li, S. An, and Y. Cai, *J. Anal. At. Spectrom.*, 2023, **38**, 142-155. https://doi.org/10.1039/d2ja00339b
46. W. Song, C. Zhu, H. Wen, Y. Zhang, Z. Liu, and M. Zhou, *Geostand. Geoanal. Res.*, 2024, 49, 245-258. https://doi.org/10.1111/ggr.12590
47. J. F. Rudge, B. C. Reynolds, and B. Bourdon, *Chem. Geol.*, 2009, **265**, 420-431. https://doi.org/10.1016/j.chemgeo.2009.05.010
48. L. P. Feng, W. Hu, Y. Jiao, L. Zhou, W. Zhang, Z. C. Hu, and Y. S. Liu, *J. Anal. At. Spectrom.*, 2020, **35**, 736-745. https://doi.org/10.1039/C9JA00385A
49. S. Eroglu, F. Scholz, M. Frank, and C. Siebert, *Geochim. Cosmochim. Acta*, 2020, **273**, 51-69. https://doi.org/10.1016/j.gca.2020.01.009
50. E. K. King, A. Thompson, O. A. Chadwick, and J. C. Pett-Ridge, *Chem. Geol.*, 2016, **445**, 54-67. https://doi.org/10.1016/j.chemgeo.2016.01.024